

A COMPARATIVE STUDY OF A CLASS OF LINEAR AND NONLINEAR PANTOGRAPH DIFFERENTIAL EQUATIONS VIA DIFFERENT ORTHOGONAL POLYNOMIAL WAVELETS

Ashish Rayal^{1a*}, Prerak A Patel^{2b}, Shailendra Giri^{3c}, Pawan Joshi^{4d}

Abstract: We propose a wavelet approach on different orthogonal polynomials for solving linear and nonlinear pantograph equations with stretch kind. The pantograph differential equation is a unique proportional delay functional differential equation class. It has been used to deal with numerous physics, mathematics, and engineering applications, such as quantum mechanics, control systems, electrodynamics, and number theory. This scheme is based on constructing the operational matrix for integration via different wavelets with their collocation nodes. This study aims to examine the numerical dynamics of the pantograph equation under stretch kind through different orthogonal polynomial wavelets. Illustrative examples are presented to highlight the flexibility of this scheme, and comparisons are made between the mentioned scheme and other existing schemes using tables and graphs. These numerical results correctly predict the applicability and effectiveness of the mentioned scheme.

Keywords: Pantograph differential equation, muntz wavelets, chebyshev wavelets of different kinds, operational matrix, collocation nodes.

1. Introduction

In variant mathematical modeling, delay differential equations (DEs) are key in solving various problems. Moreover, delay DEs are also used extensively in a distinct range of real-world situations such as economy, physiological and pharmaceutical kinetics, population dynamics, infectious diseases, chemical kinetics, epidemiology, ship navigational control, hydraulic network, etc. (Fox, 1971; Driver, 1977; Baker et al., 1995). Pantograph equation is a unique and special time delay DE that arises in several branches of applied and pure mathematics like number theory, quantum mechanics, dynamic systems, electrodynamics, control system, probability, and many more (Drfel and Iserles, 1997; Saadatmandi and Dehghan, 2009; Yusufoglu, 2010). In particular, Ockendon and Tayler (1971) and Tayler (1986) formulated this equation to describe how electricity is gathered through the pantograph of electrical locomotive. Figure 1 shows the pantograph model.

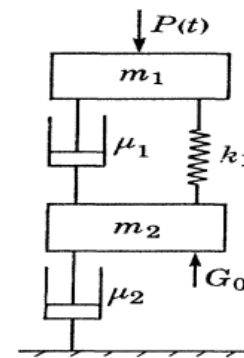


Figure 1. Pantograph Model (Ockendon and Tayler, 1971)

In this manuscript, we handle pantograph differential equation of stretch kind (PDESK) of the following form:

$$\frac{d}{dt}y(t) = g(y(\lambda t), y(t), t), \quad 0 < \lambda \in \mathbb{R} < 1, \quad t \in [0,1],$$

with the condition

$$y(0) = r_0,$$

where r_0 is the real constant, and λ is a stretched argument. The given problem is an initial value problem. In general form, we can write the above problem as

$$G\left(\frac{d}{dt}y(t), y(\lambda t), y(t), t\right) = 0, \quad (1)$$

with the condition

$$y(0) = r_0, \quad (2)$$

Authors information:

^aDepartment of Mathematics, School of Applied and Life Sciences, Uttarakhand University, Dehradun, 248007, Uttarakhand, INDIA. E-mail: ashish1989rayal@gmail.com¹

^bGujarat Power Engineering & Research Institute, Gujarat Technological University, Mehsana, Gujarat, INDIA. E-mail: patelprerak111@gmail.com²

^cDepartment of Mathematics, Education Department, Govt of Uttarakhand, Pauri Garhwal-246001, INDIA. E-mail: shailly7777@gmail.com³

^dDepartment of Applied Sciences, Shivalik college of Engineering, Dehradun-248197, INDIA. E-mail: pawan.joshi@sce.org.in⁴

*Corresponding Author: ashish1989rayal@gmail.com

Received: January 16, 2023

Accepted: July 13, 2023

Published: June 30, 2024

Various numerical approaches are based on existing orthogonal functions to solve the pantograph DEs. An overview of these approaches can be analyzed in the following studies: Sezer and Dascioglu (2007), Alomari et al. (2009), Yalcinbas et al. (2011), Sedaghat et al. (2012), Anakira et al. (2013), Tohidi et al. (2013), Yalcinbas et al. (2013), Bahsi and Cevik (2015), Jayadi et al. (2016), Yang (2018), Wang et al. (2019), Jafari et al. (2021), and Asma et al. (2022). In this study, we are interested in solving the PDESK defined in Eqs. (1-2) using wavelets based on different orthogonal functions.

In recent years, wavelets have become a growing and new area in physics, engineering, and mathematics. Wavelet analysis is a robust mathematical concept broadly used in image processing, signal processing, quantum field theory, numerical analysis, and several others (Daubechies, 1988; Mallat, 2018). Today, most physics models are analyzed through wavelet approaches. Due to the better precision of wavelets over other techniques, many researchers in different fields are interested in wavelets-based approaches (Raya and Verma, 2020a; Raya and Verma, 2020b; Raya and Verma, 2020c; Raya and Verma, 2022; Raya et al., 2022; Raya, 2023a; Raya et al., 2023b). The most popular related techniques are the Legendre wavelets method (Hafshejani et al., 2011), Laguerre wavelets method (Shiralashetti et al., 2016), Hermite wavelets scheme (Saeed and Rehman,

2014), Bernoulli wavelets scheme (Rahimkhani et al., 2016), Gegenbauer wavelets method (Muhammad et al., 2017), Mamadu-Njoseh wavelets scheme (Raya et al., 202, and Muntz wavelets scheme (Raya, 2023d).

This study aims to compute the continuous approximate solutions of the PDESK defined in Eq. (1) using different orthogonal polynomial wavelets. An approximation scheme is introduced based on different orthogonal polynomial wavelets with integral operational matrix (IOM) and collocation grids to solve PDESK. The scheme converts the problems into simultaneous algebraic equations by expressing an unknown function $y(t)$ in a truncated wavelet series. The wavelet characteristics, collocation technique, and integral operational matrix are utilized to evaluate $y(t)$ in the given problem.

This manuscript is framed as follows: Section 2 introduces different orthogonal polynomial wavelets. Section 3 describes the function approximation through wavelets series. Section 4 explains the IOM for different wavelets. Section 5 proposes an approximate scheme for solving the problem. Section 6 estimates the errors to check the accuracy of the mentioned scheme. Section 7 contains examples of predicting the efficiency and precision of the proposed technique. Section 8 summarizes this study.

2. Orthogonal Polynomial Wavelets

This section defines the wavelets based on different orthogonal polynomials.

Muntz Wavelets

The definition of Muntz wavelets (MWs) on $[0,1]$ for $\gamma \in (0,1)$ is as follows (Bahmanpour, 2018):

$$\psi_{n,m}(t) = \begin{cases} \sqrt{\frac{1}{2} + m\gamma} 2^{\frac{k}{2}} P_m(2^{k-1}t - (n-1), \gamma), & \frac{n-1}{2^{k-1}} \leq t < \frac{n}{2^{k-1}}, \\ 0, & \text{elsewhere} \end{cases}$$

where $n = 0,1,2,3, \dots, M-1$, $n = 1,2,3, \dots, 2^{k-1}$, k, M are natural numbers. The term $\sqrt{\frac{1}{2} + m\gamma}$ is employed for normality and $P_m(t)$ represents the Muntz functions of degree m that are orthogonal, corresponding to the unit weighted function $w(t)$ on $[0,1]$ and is represented in the following form:

$$P_m(t, \gamma) = \sum_{k=0}^m c_{m,k} t^{\gamma k},$$

where

$$c_{m,k} = \frac{(-1)^{m-k}}{\gamma^m k! (m-k)!} \prod_{i=0}^{m-1} ((k+i)\gamma + 1).$$

The MWs set is orthogonal under the weighted function, $w_n(t) = w(2^{k-1}t - n + 1)$.

Chebyshev Wavelets of The First Kind

The first kind of Chebyshev wavelets (CWs) have the arguments $\psi(n, m, k, t)$, in which $n = 1,2,3, \dots, 2^k$, $m = 0,1,2, \dots, M-1$ is the order for first Chebyshev functions, $k \in \mathbb{N}$ and t represents the normalized time.

The definition of the CWs on $[0,1]$ is provided as (Tavassoli, 2009):

$$\psi_{n,m}(t) = \begin{cases} \frac{\alpha_m}{\sqrt{\pi}} 2^{\frac{k}{2}} T_m(2^{k+1}t - (2n - 1)), & \frac{n-1}{2^k} \leq t < \frac{n}{2^k}, \\ 0, & \text{elsewhere} \end{cases}$$

where

$$\alpha_m = \begin{cases} \sqrt{2} & m = 0 \\ 2 & m = 1, 2, 3, \dots \end{cases}$$

Here, coefficient $\alpha_m/\sqrt{\pi}$ is employed for orthonormality and $T_m(t)$ is the first kind of Chebyshev function of degree m that is orthogonal under the weighted function $w(t) = 1/\sqrt{1-t^2}$ on $[-1,1]$ and has the following iterative relation:

$$\begin{aligned} T_0(t) &= 1, \\ T_1(t) &= t, \\ T_{m+1}(t) &= 2t T_m(t) - T_{m-1}(t), \quad m = 1, 2, \dots \end{aligned}$$

The set of CWs is orthogonal under the weighted function, $w_n(t) = w(2^{k+1}t - 2n + 1)$.

Chebyshev Wavelets of the Second Kind

The second kind of Chebyshev wavelets (SCWs) have the arguments $\psi(n, m, k, t)$ in which $n = 1, 2, 3, \dots, 2^{k-1}$, $m = 0, 1, 2, 3, \dots, M - 1$ is the order for the second Chebyshev functions, $k \in \mathbb{N}$ and t represents the normalized time.

The definition of SCWs on $[0,1]$ is provided as (Zhu and Wang, 2013):

$$\psi_{n,m}(t) = \begin{cases} \sqrt{\frac{2}{\pi}} 2^{\frac{k}{2}} U_m(2^k t - 2n + 1), & \frac{n-1}{2^{k-1}} \leq t < \frac{n}{2^{k-1}}, \\ 0, & \text{elsewhere} \end{cases}$$

Here, the term $\sqrt{2/\pi}$ is employed for normality and $U_m(t)$ is the second kind of Chebyshev function of degree m that is orthogonal under the weighted function $w(t) = \sqrt{1-t^2}$ on $[-1,1]$ and has the following iterative relation:

$$\begin{aligned} U_0(t) &= 1, \\ U_1(t) &= 2t, \\ U_{m+1}(t) &= 2t U_m(t) - U_{m-1}(t), \quad m = 1, 2, 3, \dots \end{aligned}$$

The set of SCWs is orthogonal under the weighted function. $w_n(t) = w(2^k t - 2n + 1)$.

Chebyshev Wavelets of the Third Kind

The third kind of Chebyshev wavelets (TCWs) have the arguments $\psi(n, m, k, t)$ in which $n = 1, 2, 3, \dots, 2^{k-1}$, $m = 0, 1, 2, 3, \dots, M - 1$ is the order for the third kind Chebyshev functions, $k \in \mathbb{N}$ and t represents the normalized time.

The definition of TCWs on $[0,1]$ is provided as (Polat, 2019):

$$\psi_{n,m}(t) = \begin{cases} \frac{1}{\sqrt{\pi}} 2^{\frac{k}{2}} V_m(2^k t - 2n + 1), & \frac{n-1}{2^{k-1}} \leq t < \frac{n}{2^{k-1}}, \\ 0, & \text{elsewhere} \end{cases}$$

Here, the coefficient $\sqrt{1/\pi}$ is used for normality and $V_m(t)$ is the third Chebyshev function of degree m that is orthogonal under the weighted function $w(t) = \frac{\sqrt{1+t}}{\sqrt{1-t}}$ on $[-1,1]$ and has the following iterative relation:

$$\begin{aligned} V_0(t) &= 1, \\ V_1(t) &= 2t - 1, \\ V_{m+1}(t) &= 2t V_m(t) - V_{m-1}(t), \quad m = 1, 2, 3, \dots \end{aligned}$$

The set of TCWs is orthogonal under the weighted function, $w_n(t) = w(2^k t - 2n + 1)$.

Chebyshev Wavelets of the Fourth Kind

The fourth kind of Chebyshev wavelets (FCWs) have the arguments $\psi(n, m, k, t)$ in which $n = 1, 2, 3, \dots, 2^{k-1}$, $m = 0, 1, 2, 3, \dots, M - 1$ is the order for the fourth kind Chebyshev functions, $k \in \mathbb{N}$ and t represents the normalized time.

The definition of FCWs on $[0,1]$ is as follows (Azodi and Yaghouti, 2018):

$$\psi_{n,m}(t) = \begin{cases} \frac{1}{\sqrt{\pi}} 2^{\frac{k}{2}} W_m(2^k t - (2n - 1)), & \frac{n-1}{2^{k-1}} \leq t < \frac{n}{2^{k-1}}, \\ 0, & \text{elsewhere} \end{cases}$$

Here, the coefficient $1/\sqrt{\pi}$ is used for normality and $W_m(t)$ is the fourth Chebyshev function of degree m that is orthogonal under the weighted function $w(t) = \sqrt{\frac{1-t}{1+t}}$ on $[-1,1]$ and has the following iterative relation:

$$\begin{aligned} W_0(t) &= 1, \\ W_1(t) &= 2t + 1, \\ W_{m+1}(t) &= 2t W_m(t) - W_{m-1}(t), \quad m = 1, 2, 3, \dots \end{aligned}$$

The set of CWs is orthogonal under the weighted function, $w_n(t) = w(2^k t - 2n + 1)$.

Now, the wavelet function approximation is described in the successive sections using the considered wavelet basis functions.

3. Function Approximation

A function $h(t)$ on $[0,1]$ can be approximated via considered wavelets as

$$h(t) \approx \sum_{n=1}^{\infty} \sum_{m=0}^{\infty} e_{n,m} \psi_{n,m}(t), \tag{3}$$

where $e_{n,m}$ are computed by

$$e_{n,m} = \langle h(t), \psi_{n,m} \rangle_{w_n(t)} = \int_0^1 h(t) \psi_{n,m}(t) w_n(t) dt$$

Here, the notation $\langle \cdot, \cdot \rangle$ describes the inner product in $L^2[0,1]$ with the weighted function $w_n(t)$. The truncated form of Eq. (3) is rewritten as:

$$h(t) \approx \sum_{n=1}^{2^{k-1}} \sum_{m=0}^{M-1} e_{n,m} \psi_{n,m}(t) = E^T \Psi(t) = \Psi^T(t) E, \tag{4}$$

where E and $\Psi(t)$ are provided by

$$\begin{aligned} E &= [e_{1,0}, \dots, e_{1,(M-1)}, e_{2,0}, \dots, e_{2,(M-1)}, \dots, e_{2^{k-1},0}, \dots, e_{2^{k-1},(M-1)}]^T \\ &= [e_1, e_2, \dots, e_{\hat{m}}]^T, \end{aligned} \tag{5}$$

$$\begin{aligned} \Psi(t) &= \begin{bmatrix} \psi_{1,0}(t), \dots, \psi_{1,(M-1)}(t), \psi_{2,0}(t), \dots, \psi_{2,(M-1)}(t), \dots, \\ \psi_{2^{k-1},0}(t), \dots, \psi_{2^{k-1},(M-1)}(t) \end{bmatrix}^T \\ &= [\psi_1, \psi_2, \dots, \psi_{\hat{m}}]^T. \end{aligned} \tag{6}$$

Here, $\hat{m} = 2^{k-1}M$ denotes the total considered wavelets basis, but in the case of the first kind of Chebyshev wavelets $\hat{m} = 2^k M$.

4. Integral Operational Matrix for Orthogonal Polynomial Wavelets

This section provides the IOM $P_{\hat{m} \times \hat{m}}$ for different wavelets that play an important part in the PDESK solution. This operational matrix is employed to transform the given model to the algebraic system of equations in terms of wavelet coefficient. By applying the IOM, a large unknown coefficient vector does not occur when computing the numerical approximation of a linear and nonlinear PDESK class. Consequently, the calculations are made simple, resulting in better solution accuracy. In general,

$$\int_0^t \Psi(t) dt \approx P_{\hat{m} \times \hat{m}} \Psi(t), \tag{7}$$

where $\Psi(t)$ is provided in Eq. (6) and $P_{\hat{m} \times \hat{m}}$ is the IOM determined by

$$P_{\hat{m} \times \hat{m}} = \langle g_{\hat{m} \times 1}(t), \Psi_{\hat{m} \times 1}^T(t) \rangle_{w_n(t)},$$

where

$$g_{\hat{m} \times 1}(t) = \int_0^t \Psi(t) dt$$

and the notation $\langle . . . \rangle$ represents the inner product in $L^2[0,1]$ under the weighted function $w_n(t)$.

Using Eq. (7), construct the following IOM for different wavelets:

- (a) The IOM of the Muntz wavelets ($\gamma = 0.5, k = 1, M = 8$):

$$(P_{8 \times 8})_{MWS} = \begin{bmatrix} \frac{1}{2} & \frac{\sqrt{2}}{5} & \frac{1}{10\sqrt{3}} & 0 & 0 & 0 & 0 & 0 \\ -\frac{\sqrt{2}}{5} & 0 & \frac{\sqrt{2}}{7\sqrt{3}} & \frac{\sqrt{2}}{35} & 0 & 0 & 0 & 0 \\ -\frac{1}{10\sqrt{3}} & -\frac{\sqrt{2}}{7\sqrt{3}} & 0 & \frac{2}{15\sqrt{3}} & \frac{\sqrt{5}}{42\sqrt{3}} & 0 & 0 & 0 \\ 0 & -\frac{\sqrt{2}}{35} & -\frac{2}{15\sqrt{3}} & 0 & \frac{2\sqrt{5}}{77} & \frac{\sqrt{2}}{33\sqrt{3}} & 0 & 0 \\ 0 & 0 & -\frac{\sqrt{5}}{42\sqrt{3}} & -\frac{2\sqrt{5}}{77} & 0 & \frac{\sqrt{10}}{39\sqrt{3}} & \frac{\sqrt{35}}{286} & 0 \\ 0 & 0 & 0 & -\frac{\sqrt{2}}{33\sqrt{3}} & -\frac{\sqrt{10}}{39\sqrt{3}} & 0 & \frac{\sqrt{14}}{55\sqrt{3}} & \frac{2}{65\sqrt{3}} \\ 0 & 0 & 0 & 0 & -\frac{\sqrt{35}}{286} & -\frac{\sqrt{14}}{55\sqrt{3}} & 0 & \frac{2\sqrt{14}}{221} \\ 0 & 0 & 0 & 0 & 0 & -\frac{2}{65\sqrt{3}} & -\frac{2\sqrt{14}}{221} & 0 \end{bmatrix};$$

(b) The IOM of the first kind of Chebyshev wavelets ($k = 0, M = 8$):

$$(\mathbf{P}_{8 \times 8})_{\text{CWS}} = \begin{bmatrix} \frac{1}{2} & \frac{1}{2\sqrt{2}} & 0 & 0 & 0 & 0 & 0 & 0 \\ -\frac{1}{4\sqrt{2}} & 0 & \frac{1}{8} & 0 & 0 & 0 & 0 & 0 \\ -\frac{1}{3\sqrt{2}} & -\frac{1}{4} & 0 & \frac{1}{12} & 0 & 0 & 0 & 0 \\ \frac{1}{8\sqrt{2}} & 0 & -\frac{1}{8} & 0 & \frac{1}{16} & 0 & 0 & 0 \\ -\frac{1}{15\sqrt{2}} & 0 & 0 & -\frac{1}{12} & 0 & \frac{1}{20} & 0 & 0 \\ \frac{1}{24\sqrt{2}} & 0 & 0 & 0 & -\frac{1}{16} & 0 & \frac{1}{24} & 0 \\ -\frac{1}{35\sqrt{2}} & 0 & 0 & 0 & 0 & -\frac{1}{20} & 0 & \frac{1}{28} \\ \frac{1}{48\sqrt{2}} & 0 & 0 & 0 & 0 & 0 & -\frac{1}{24} & 0 \end{bmatrix};$$

(c) The IOM of second kind Chebyshev wavelets ($k = 1, M = 8$):

$$(\mathbf{P}_{8 \times 8})_{\text{SCWS}} = \begin{bmatrix} \frac{1}{2} & \frac{1}{4} & 0 & 0 & 0 & 0 & 0 & 0 \\ -\frac{3}{8} & 0 & \frac{1}{8} & 0 & 0 & 0 & 0 & 0 \\ \frac{1}{6} & -\frac{1}{12} & 0 & \frac{1}{12} & 0 & 0 & 0 & 0 \\ -\frac{1}{8} & 0 & -\frac{1}{16} & 0 & \frac{1}{16} & 0 & 0 & 0 \\ \frac{1}{10} & 0 & 0 & -\frac{1}{20} & 0 & \frac{1}{20} & 0 & 0 \\ -\frac{1}{12} & 0 & 0 & 0 & -\frac{1}{24} & 0 & \frac{1}{24} & 0 \\ \frac{1}{14} & 0 & 0 & 0 & 0 & -\frac{1}{28} & 0 & \frac{1}{28} \\ -\frac{1}{16} & 0 & 0 & 0 & 0 & 0 & -\frac{1}{32} & 0 \end{bmatrix};$$

(d) The IOM of third kind Chebyshev wavelets ($k = 1, M = 8$):

$$(\mathbf{P}_{8 \times 8})_{\text{TCWs}} = \begin{bmatrix} \frac{3}{4} & \frac{1}{4} & 0 & 0 & 0 & 0 & 0 & 0 \\ -1 & -\frac{1}{8} & \frac{1}{8} & 0 & 0 & 0 & 0 & 0 \\ \frac{5}{12} & -\frac{1}{8} & -\frac{1}{24} & \frac{1}{12} & 0 & 0 & 0 & 0 \\ -\frac{7}{24} & 0 & -\frac{1}{12} & -\frac{1}{48} & \frac{1}{16} & 0 & 0 & 0 \\ \frac{9}{10} & 0 & 0 & -\frac{1}{16} & -\frac{1}{80} & \frac{1}{20} & 0 & 0 \\ -\frac{11}{60} & 0 & 0 & 0 & -\frac{1}{20} & -\frac{1}{120} & \frac{1}{24} & 0 \\ \frac{13}{84} & 0 & 0 & 0 & 0 & -\frac{1}{24} & -\frac{1}{168} & \frac{1}{28} \\ -\frac{15}{112} & 0 & 0 & 0 & 0 & 0 & -\frac{1}{28} & -\frac{1}{224} \end{bmatrix};$$

(e) The IOM of fourth kind Chebyshev wavelets ($k = 1, M = 8$):

$$(\mathbf{P}_{8 \times 8})_{\text{FCWs}} = \begin{bmatrix} \frac{1}{4} & \frac{1}{4} & 0 & 0 & 0 & 0 & 0 & 0 \\ 0 & \frac{1}{8} & \frac{1}{8} & 0 & 0 & 0 & 0 & 0 \\ -\frac{1}{12} & -\frac{1}{8} & \frac{1}{24} & \frac{1}{12} & 0 & 0 & 0 & 0 \\ \frac{1}{24} & 0 & -\frac{1}{12} & \frac{1}{48} & \frac{1}{16} & 0 & 0 & 0 \\ -\frac{1}{40} & 0 & 0 & -\frac{1}{16} & \frac{1}{80} & \frac{1}{20} & 0 & 0 \\ \frac{1}{60} & 0 & 0 & 0 & -\frac{1}{20} & \frac{1}{120} & \frac{1}{24} & 0 \\ -\frac{1}{84} & 0 & 0 & 0 & 0 & -\frac{1}{24} & \frac{1}{168} & \frac{1}{28} \\ \frac{1}{112} & 0 & 0 & 0 & 0 & 0 & -\frac{1}{28} & \frac{1}{224} \end{bmatrix};$$

The next section explores the numerical PDESK solutions.

5. Formulation of the Method

This section presents an approximate method based on orthogonal polynomial wavelets. The procedure of applying the method to a given problem is as follows.

Take the model equation from Eqs. (1-2) and expand the function, $\frac{d}{dt}y(t)$ via truncated series of wavelets over the interval [0,1] as

$$\frac{d}{dt}y(t) \approx E^T \Psi(t), \tag{8}$$

where E and $\Psi(t)$ are provided in Eqs. (5) and (6) respectively. By integrating Eq. (8) from 0 to t , we get

$$y(t) \approx E^T \int_0^t \Psi(t) dt + y(0) = E^T P_{\hat{m} \times \hat{m}} \Psi(t),$$

where $P_{\hat{m} \times \hat{m}}$ is the IOM of wavelets given in Eq. (7). After simplification, we obtain

$$\begin{aligned} y(t) &\approx E^T P_{\hat{m} \times \hat{m}} \Psi(t) + y(0) \\ &= E^T P_{\hat{m} \times \hat{m}} \Psi(t) + r_0 \\ &= E^T P_{\hat{m} \times \hat{m}} \Psi(t) + d^T \Psi(t) \\ &= (E^T P_{\hat{m} \times \hat{m}} + d^T) \Psi(t) = y_{\hat{m}}(t), \end{aligned} \tag{9}$$

where vector d is chosen as:

$$d^T \Psi(t) = r_0. \tag{10}$$

By using an approximation form of function $y(t)$ given in Eq. (9), we obtain $y(\lambda t)$ as

$$y(\lambda t) \approx (E^T P_{\hat{m} \times \hat{m}} + d^T) \Psi(\lambda t), \tag{11}$$

where $\Psi(\lambda t)$ is a stretched wavelets function. Using Eqs. (8-10) into Eq. (1), we obtain:

$$G(E^T \Psi(t), (E^T P_{\hat{m} \times \hat{m}} + d^T) \Psi(\lambda t), (E^T P_{\hat{m} \times \hat{m}} + d^T) \Psi(t), t) = 0. \tag{12}$$

Now, collocating the obtained system at the appropriate grids t_i :

$$G(E^T \Psi(t_i), (E^T P_{\hat{m} \times \hat{m}} + d^T) \Psi(\lambda t_i), (E^T P_{\hat{m} \times \hat{m}} + d^T) \Psi(t_i), t_i) = 0, \tag{13}$$

where

$$t_i = \frac{2i - 1}{2^k M}, \quad i = 1, 2, \dots, 2^{k-1} M. \tag{14}$$

The resultant algebraic set in Eq. (13) can be evaluated properly for wavelet coefficients E . Finally, the solution $y_{\hat{m}}(t)$ of the given problem is achieved through the inclusion of estimated coefficient E into Eq. (9) as $y_{\hat{m}}(t) = (E^T P_{\hat{m} \times \hat{m}} + d^T) \Psi(t)$.

Figure 2 displays the flowchart for implementing the constructed scheme.

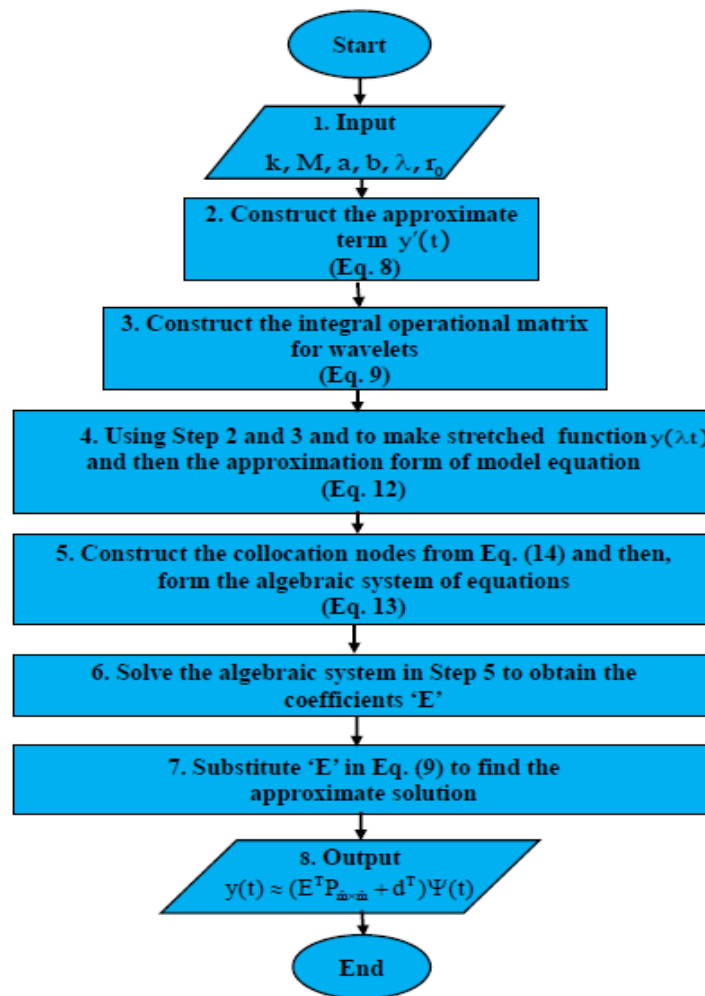


Figure 2. Flowchart for implementing the constructed scheme

6. Error Estimation of Solution

This section provides the convergence formulae to analyze the errors in the computation results. To investigate the accuracy of the proposed method, we define the error formulae as:

(a) Let $y_{\hat{m}}(t)$ be the estimate solution to $y(t)$ of Eqs. (1-2). Then $E_{Abs}(t)$ at $t \in [0,1]$ is calculated as

$$E_{Abs}(t) = |y(t) - y_{\hat{m}}(t)|,$$

where $y(t)$ is the analytical solution of the considered model.

(b) L_{∞} , the maximum absolute error is computed by

$$L_{\infty} = \max_{t \in [0,1]} |E_{Abs}(t)|$$

(c) The L^2 norm consecutive error ($\mathcal{C}.\mathcal{E}$) is computed by

$$\mathcal{C}.\mathcal{E} = \|y_{\hat{m}+1}(t) - y_{\hat{m}}(t)\|_2, \quad t \in [0,1]. \tag{15}$$

(d) The reliability of the results and accuracy of the scheme can be checked through residual error function in the absence of an exact solution of the proposed model as:

$$E_{\hat{m}}(t) = \left| \frac{d}{dt} y_{\hat{m}}(t) - g(y_{\hat{m}}(\lambda t), y_{\hat{m}}(t), t) \right|, \quad t \in [0,1]$$

If $E_{\hat{m}}(t) \rightarrow 0$ for \hat{m} , then the error decreases.

7. Method Implementation

This section implements the constructed scheme with MWs, CWs, SCWs, TCWs, and FCWs to solve PDESK, and the approximated outputs obtained are compared with the corresponding available analytical solution. The L^2 norm consecutive errors and absolute errors demonstrate the accuracy of the constructed scheme. The proposed method is easy to implement, but the computational cost may be complex. All numerical outputs are computed using Mathematica.

Example 1.

Consider the PDESK (Bellen & Zennaro, 2003) as:

$$\frac{d}{dt}y(t) = y(0.5t), \quad 0 \leq t \leq 1,$$

with the condition

$$y(0) = 1$$

The closed-form solution of the considered example is provided (Bellen & Zennaro, 2003):

$$y(t) = \sum_{j=0}^{\infty} \frac{1}{j!} (2)^{\frac{j(1-j)}{2}} t^j.$$

We solve the above example for $\hat{m} = 8$ using the scheme introduced in Section 5. The wavelet coefficient vector of $y(t)$ can be determined as:

$$y_{MWs}(t) = 1.0 + 0.0000109285\sqrt{t} + 0.99986t + 0.000833015t^{1.5} + 0.24731t^2 + 0.0049748t^{2.5} + 0.0155824t^3 + 0.00292117t^{3.5}.$$

$$y_{CWs}(t) = 1.0 + t + 0.25t^2 + 0.0208333t^3 + 0.000651042t^4 + 8.13802 \times 10^{-6}t^5 + 4.23849 \times 10^{-8}t^6 + 9.49902 \times 10^{-11}t^7.$$

$$y_{SCWs}(t) = 1.0 + t + 0.25t^2 + 0.0208333t^3 + 0.000651042t^4 + 8.13802 \times 10^{-6}t^5 + 4.2385 \times 10^{-8}t^6 + 9.4948 \times 10^{-11}t^7.$$

$$y_{TCWs}(t) = 1.0 + t + 0.25t^2 + 0.0208333t^3 + 0.000651042t^4 + 8.13802 \times 10^{-6}t^5 + 4.23847 \times 10^{-8}t^6 + 9.50405 \times 10^{-11}t^7.$$

$$y_{FCWs}(t) = 1.0 + t + 0.25t^2 + 0.0208333t^3 + 0.000651042t^4 + 8.13802 \times 10^{-6}t^5 + 4.23854 \times 10^{-8}t^6 + 9.48487 \times 10^{-11}t^7.$$

Figures 3 and 4 display the achieved solutions and corresponding errors via different wavelets. Tables 1 and 2 present the approximate wavelet solutions through different wavelets with an exact solution and the Legendre wavelets method (LWM) (Hafshejani et al., 2011). One may observe from the tables and figures that the wavelet solutions converge faster to the analytical result. The error decreases more rapidly when the number of basic functions increases. Table 3 shows the L^2 norm consecutive error for the order of approximation $\hat{m} = 7,8$. Table 3 confirms that the error decreases with the increase of the order of approximation \hat{m} , which shows the accuracy of the described scheme. The L^2 norm consecutive error is calculated for the first time in this study using Eq. (15).

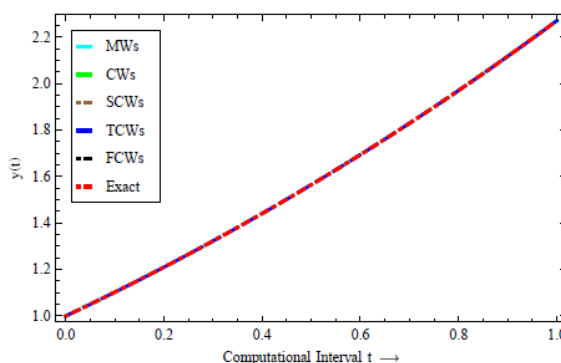


Figure 3. The behavior of the estimated solutions for different wavelets with $\hat{m} = 8$ in Example 1

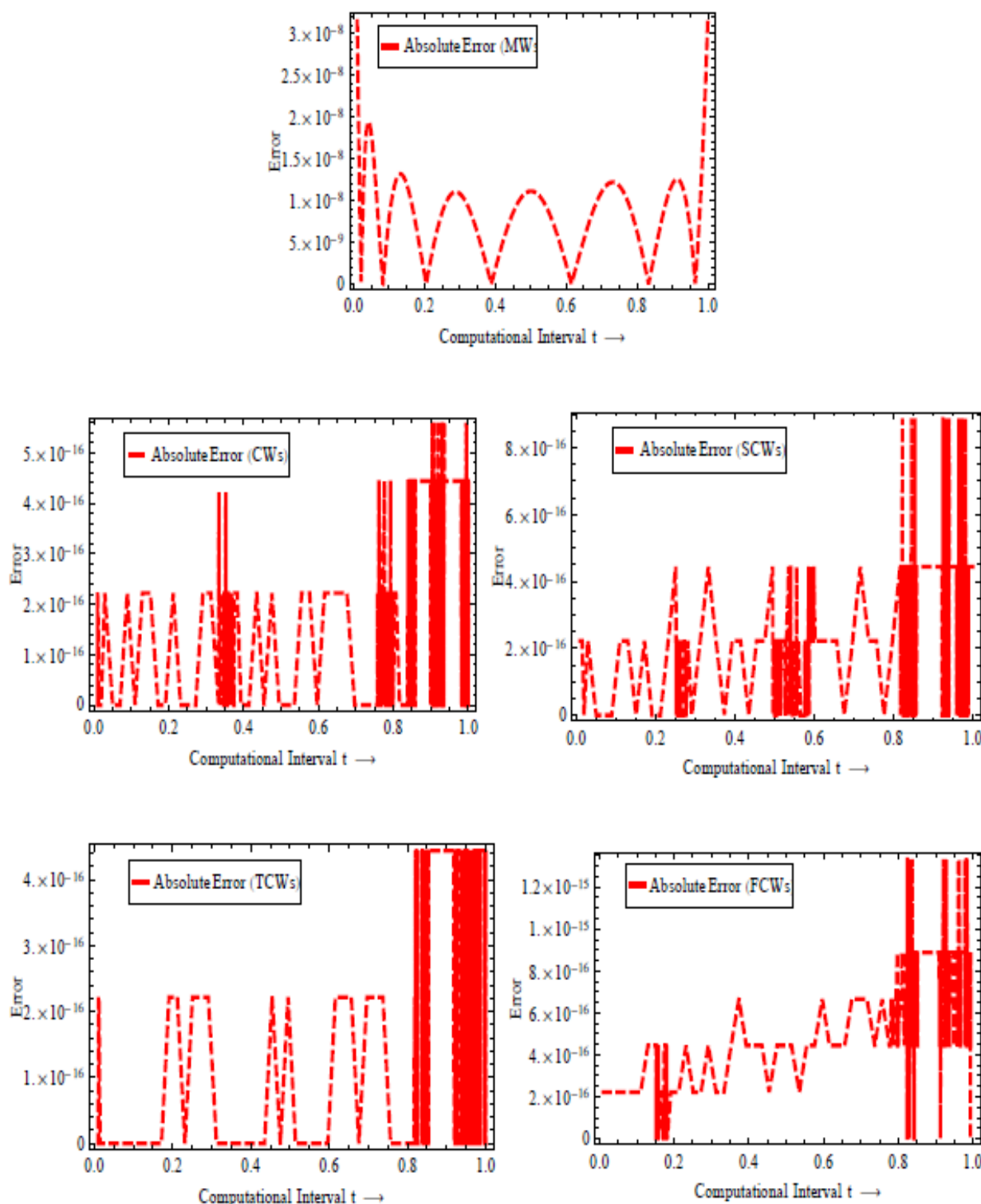


Figure 4. Absolute errors of the solutions via different wavelets with $\hat{m} = 8$ in Example 1

Table 1. Computed values of $y(t)$ via the constructed approach compared to Example 1

t	LWs (Hafshejani et al., 2011), $\hat{m} = 18$	Present Method (MWs), $\hat{m} = 8$	Exact Solution
0.000	0.999999999999999	0.999999725312605	1.000000000000000
0.125	1.12894709929840	1.128947112205302	1.1289470992984005
0.250	1.26595307192248	1.265953063336836	1.2659530719224836
0.375	1.41126781788344	1.411267815667616	1.4112678178834435
0.500	1.56514511174700	1.565145122864885	1.5651451117469977
0.625	1.72784263272750	1.727842631181262	1.7278426327275054
0.750	1.89962199489918	1.899621983149178	1.8996219948991855
0.875	2.08074877752466	2.080748786130356	2.0807487775246620
1.000	2.27149255550106	2.271492523809371	2.2714925555010614

Table 2. Approximated values of $y(t)$ via constructed scheme in Example 1

t	Present method (CWs), $\hat{m} = 8$	Present method (SCWs), $\hat{m} = 8$	Present method (TCWs), $\hat{m} = 8$	Present method (FCWs), $\hat{m} = 8$
0.000	1.000000000000000	1.000000000000000	0.999999999999999	1.000000000000000
0.125	1.1289470992984003	1.1289470992984005	1.1289470992984005	1.1289470992984003
0.250	1.2659530719224834	1.2659530719224836	1.2659530719224836	1.2659530719224834
0.375	1.4112678178834435	1.4112678178834437	1.4112678178834435	1.4112678178834432
0.500	1.5651451117469974	1.5651451117469979	1.5651451117469979	1.5651451117469972
0.625	1.7278426327275052	1.7278426327275054	1.7278426327275054	1.7278426327275047
0.750	1.8996219948991855	1.8996219948991860	1.8996219948991855	1.8996219948991848
0.875	2.0807487775246620	2.0807487775246620	2.0807487775246620	2.0807487775246614
1.000	2.2714925555010614	2.2714925555010620	2.2714925555010614	2.2714925555010610

Table 3. Efficiency of the constructed method in the terms of L^2 norm consecutive error via different wavelets in Example 1

\hat{m}	MWs	CWs	SCWs	TCWs	FCWs
7	5.86×10^{-6}	1.49×10^{-11}	1.50×10^{-11}	2.12×10^{-11}	2.03×10^{-11}
8	1.61×10^{-7}	8.25×10^{-15}	8.30×10^{-15}	1.18×10^{-14}	1.16×10^{-14}

Example 2

Consider the linear PDESK (Yalcinbas, 2011; Bahsi & Cevik, 2015) as:

$$\frac{d}{dt}y(t) = -y(0.8t) - y(t), \quad 0 \leq t \leq 1,$$

with the condition

$$y(0) = 1.$$

There is no analytical solution to this problem. We treat this example for $\hat{m} = 8$ by using the scheme introduced in Section 5 and the wavelets series solution of $y(t)$ can be achieved as:

$$y_{MWS}(t) = 1.00007 - 0.0028539\sqrt{t} - 1.96514t - 0.193559t^{1.5} + 2.3507t^2 - 0.78919t^{2.5} - 0.59084t^3 + 0.29353t^{3.5}.$$

$$y_{CWS}(t) = 1 - 2t + 1.79997t^2 - 0.983756t^3 + 0.370964t^4 - 0.10267t^5 + 0.0204596t^6 - 0.00229864t^7.$$

$$y_{SCWS}(t) = 1 - 2t + 1.79996t^2 - 0.983709t^3 + 0.370873t^4 - 0.102583t^5 + 0.0204227t^6 - 0.00229449t^7.$$

$$y_{TCWS}(t) = 1 - 2t + 1.79994t^2 - 0.9836t^3 + 0.370581t^4 - 0.102167t^5 + 0.0201234t^6 - 0.00220884t^7.$$

$$y_{FCWS}(t) = 1 - 2t + 1.79998t^2 - 0.983827t^3 + 0.371189t^4 - 0.103032t^5 + 0.0207461t^6 - 0.00238706t^7.$$

As mentioned above, we do not know the analytical solution to the given problem. Therefore, we estimate the solutions in Table 4 and observe a convergence. A comparison of Table 4 with the solutions achieved through several schemes is displayed in Table 5 (Tohidi et al., 2013; Yalcinbas et al., 2015; Yang, 2018; Yuzbas et al., 2014; Bahsi & Cevik, 2015; Yalcinbas et al., 2011; Sezer & Akyuz-Dascioglu, 2007). The calculated approximate solutions and corresponding absolute errors are displayed in Figures 5 and 6, respectively. Table 6 shows the L^2 norm consecutive error for the order of approximation $\hat{m} = 7,8$, which clearly shows the accuracy of the constructed approach. The numerical results of the suggested method are consistent.

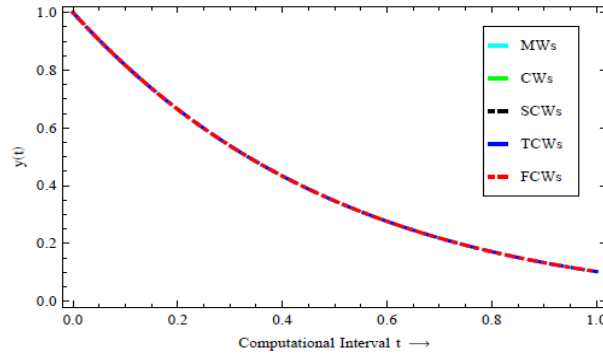


Figure 5. The behavior of the approximate wavelet solutions for different wavelets with $\hat{m} = 8$ in Example 2

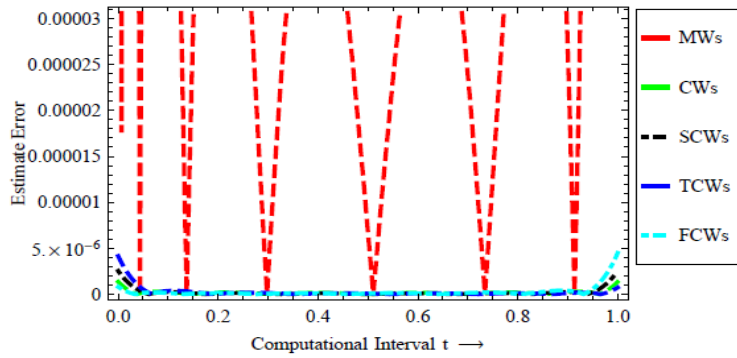


Figure 6. Estimate absolute errors of the solutions through different wavelets with $\hat{m} = 8$ in Example 2

Table 4. Approximated values of $y(t)$ with $\hat{m} = 8$ using the proposed scheme in Example 2

t	Present Method (MWs)	Present method (FCWs)	Present method (TCWs)	Present method (SCWs)	Present method (CWs)
0.0	1.0000737941	0.9999999944	0.9999999133	0.9999999523	0.9999999893
0.2	0.6646904337	0.6646910015	0.6646909898	0.6646909954	0.6646909970
0.4	0.4335604608	0.4335607737	0.4335607859	0.4335607800	0.4335607781
0.6	0.2764814550	0.2764823377	0.2764823264	0.2764823318	0.2764823311
0.8	0.1714859287	0.1714840995	0.1714841125	0.1714841063	0.1714841076
1.0	0.1026802165	0.1026700336	0.1026701212	0.1026700791	0.1026701151

Table 5. Approximated values of $y(t)$ using different schemes for comparison in Example 2

t	Bernoulli method (Tohidi et al., 2013), $\hat{m} = 7$	Bernstein method (Yalcinbas et al. 2015), $\hat{m} = 11$	Chebyshev method (Yang, 2018), $\hat{m} = 7$	Laguerre method (Yuzbas et al., 2014), $\hat{m} = 9$	PIA (1,1) (Bahsi, & Cevik, 2015)	Hermite method (Yalcinbas et al., 2011), $\hat{m} = 9$	Taylor method (Sezer & Akyuz-Dascioglu, 2007), $\hat{m} = 12$
0.0	1.0000000	1.00000000	1.00000000	1.0000000	1.0000000	1.000000	1.000000
0.2	0.6646905	0.66469100	0.66469101	0.6646910	0.6646910	0.664691	0.664691
0.4	0.4335605	0.43356077	0.43356077	0.4335607	0.4335607	0.433561	0.433561
0.6	0.2764822	0.27648233	0.27648233	0.2764831	0.2764823	0.276482	0.276482
0.8	0.1714836	0.17148411	0.17148412	0.1714942	0.1714841	0.171484	0.171484
1.0	0.1026832	0.10267012	0.10267013	0.1027437	0.1026701	0.102670	0.102670

Table 6. Efficiency of the constructed method in terms of L^2 norm consecutive error using different wavelets in Example 2

\hat{m}	MWs	CWs	SCWs	TCWs	FCWs
7	1.10×10^{-4}	4.39×10^{-6}	4.13×10^{-6}	5.33×10^{-6}	6.31×10^{-6}
8	1.61×10^{-5}	2.01×10^{-7}	1.95×10^{-7}	2.56×10^{-7}	2.93×10^{-7}

Example 3

Consider the PDESK as

$$\frac{d}{dt}y(t) = 0.95y(t) - y(0.99t), \quad 0 \leq t \leq 1,$$

with the initial condition

$$y(0) = 1.$$

There is no analytical solution to this problem. We solve it by considering the example for $\hat{m} = 8$ using the scheme introduced in Section 5. Because we do not know the analytical solution to the given problem, we show the accuracy of the described scheme by evaluating the residual error function. Table 7 shows the estimated numerical solutions via different wavelets, showing smooth convergence. Figure 7 plots the approximated solutions obtained for $\hat{m} = 8$. Figure 8 shows the graphical representation of the estimated errors in terms of residual function via different wavelets. Figure 7 shows that the approximated solution of the considered example decreases as t increases from 0 to 1. Table 8 exhibits the L^2 norm consecutive error for $\hat{m} = 7,8$. Table 8 confirms that the error decreases rapidly with increasing order of approximation, \hat{m} , which clearly shows the effectiveness of the constructed scheme.

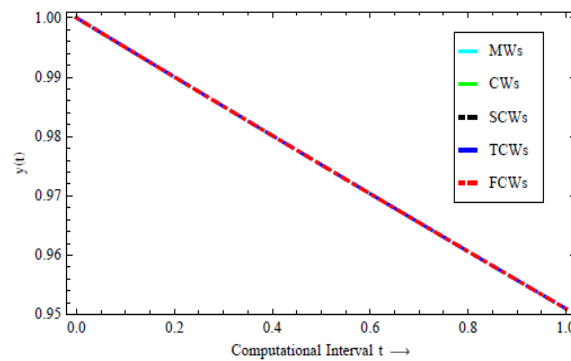


Figure 7. The behavior of the approximate solutions for different wavelets with $\hat{m} = 8$ in Example 3

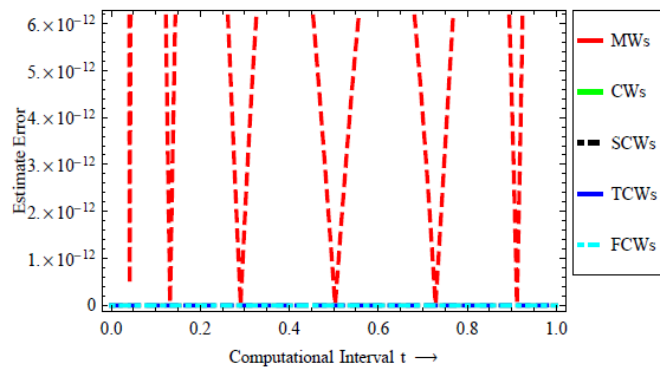


Figure 8. Error functions of the solutions using different wavelets with $\hat{m} = 8$ in Example 3

Table 7. Approximated values of $y(t)$ using the proposed scheme in Example 3

t	Present Method (MWs), $\hat{m} = 8$	Present method (CWs), $\hat{m} = 8$	Present method (SCWs), $\hat{m} = 8$	Present method (TCWs), $\hat{m} = 8$	Present method (FCWs), $\hat{m} = 8$
0.0	0.9999999999816	0.9999999999999	1.0000000000000	1.0000000000000	0.9999999999999
0.2	0.9900399198148	0.9900399198147	0.9900399198147	0.9900399198147	0.9900399198147
0.4	0.9801593591690	0.9801593591690	0.9801593591690	0.9801593591690	0.9801593591690
0.6	0.9703578393905	0.9703578393904	0.9703578393904	0.9703578393904	0.9703578393904
0.8	0.9606348837531	0.9606348837534	0.9606348837534	0.9606348837534	0.9606348837534
1.0	0.9509900174734	0.9509900174754	0.9509900174754	0.9509900174754	0.9509900174754

Table 8. Efficiency of the constructed method in terms of L^2 , norm consecutive error using different wavelets in Example 3.

\hat{m}	MWs	CWs	SCWs	TCWs	FCWs
7	2.11×10^{-9}	2.62×10^{-16}	2.36×10^{-17}	2.73×10^{-17}	1.60×10^{-16}
8	1.17×10^{-11}	2.16×10^{-16}	3.30×10^{-18}	1.33×10^{-17}	3.11×10^{-18}

Example 4.

Consider the nonlinear PDESK (Hafshejani et al., 2011; Anakira et al., 2013) as

$$\frac{d}{dt}y(t) = 1 - 2y^2\left(\frac{t}{2}\right), \quad 0 \leq t \leq 1,$$

with the condition

$$y(0) = 0.$$

The analytical solution to the example is provided as follows:

$$y(t) = \sin(t).$$

We treat this example for $\hat{m} = 8$ using the procedure given in Section 5. Figure 9 plots the approximate solutions obtained using different wavelets for $\hat{m} = 8$. Table 9 displays the estimated absolute errors using different wavelets to compare the method (Hafshejani et al., 2011). Table 10 gives the maximum absolute error for $\hat{m} = 6,7,8$. The maximum absolute errors to the same problem are 1.2×10^{-6} , 4.0×10^{-8} , 9.99×10^{-10} , and 1.2×10^{-7} (for 3 iteration), respectively (Alomari et al., 2009; Anakira et al., 2013; Hafshejani et al., 2011; Bahsi & Cevik, 2015). Table 11 exhibits the L^2 norm consecutive error for $\hat{m} = 7,8$, which confirms that the error decreases rapidly as the order of approximation \hat{m} increases.

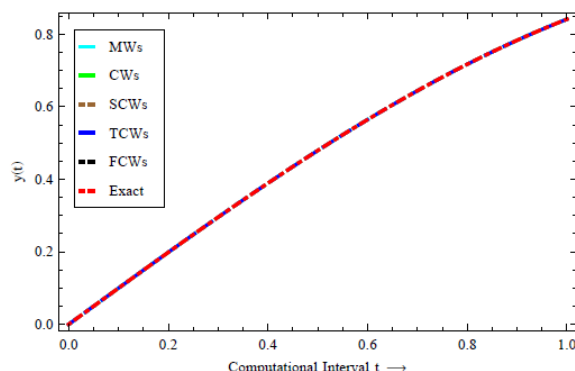


Figure 9. The behavior of the approximate solutions for different wavelets with $\hat{m} = 8$ in Example 4

Table 9. Absolute errors of $y(t)$ using the current scheme at $\hat{m} = 8$ compared to Example 4

t	MWs	CWs	SCWs	TCWs	FCWs	LWM (Hafshejani et al., 2011) $\hat{m} = 18$
0.125	9.7×10^{-6}	5.1×10^{-10}	2.5×10^{-10}	1.1×10^{-10}	3.8×10^{-10}	1.9×10^{-9}
0.250	6.6×10^{-6}	1.4×10^{-11}	1.7×10^{-10}	3.6×10^{-10}	1.6×10^{-11}	1.9×10^{-9}
0.375	6.4×10^{-6}	2.8×10^{-11}	2.8×10^{-11}	1.3×10^{-10}	1.8×10^{-10}	1.9×10^{-9}
0.500	7.3×10^{-6}	4.7×10^{-10}	2.9×10^{-10}	2.8×10^{-10}	3.1×10^{-10}	9.9×10^{-10}
0.625	5.1×10^{-6}	2.8×10^{-11}	1.3×10^{-11}	1.2×10^{-10}	1.5×10^{-10}	9.9×10^{-10}
0.750	2.9×10^{-6}	2.6×10^{-11}	1.1×10^{-10}	8.3×10^{-11}	3.0×10^{-10}	9.9×10^{-10}
0.875	4.0×10^{-6}	4.3×10^{-10}	1.3×10^{-10}	2.8×10^{-10}	1.4×10^{-11}	9.9×10^{-10}
1.000	2.7×10^{-6}	5.6×10^{-10}	1.8×10^{-9}	4.1×10^{-10}	3.2×10^{-9}	9.9×10^{-10}

Table 10. Maximum absolute error using different wavelets in Example 4

\hat{m}	MWs	CWs	SCWs	TCWs	FCWs
6	1.97×10^{-4}	2.96×10^{-7}	2.02×10^{-7}	1.36×10^{-7}	3.09×10^{-7}
7	2.59×10^{-5}	1.66×10^{-8}	7.53×10^{-9}	8.36×10^{-9}	1.30×10^{-8}
8	7.42×10^{-6}	2.20×10^{-10}	8.63×10^{-11}	3.35×10^{-10}	1.64×10^{-10}

Table 11. Efficiency of the proposed method in terms of L^2 norm consecutive error using different wavelets in Example 4

\hat{m}	MWs	CWs	SCWs	TCWs	FCWs
7	1.50×10^{-4}	2.34×10^{-7}	2.43×10^{-7}	3.46×10^{-7}	3.21×10^{-7}
8	1.22×10^{-5}	1.53×10^{-8}	1.50×10^{-8}	2.12×10^{-8}	2.11×10^{-8}

8. Conclusion

This paper proposes an approximation scheme using five orthogonal polynomial wavelets to solve PDESK. This method is examined using four problems. The error graphs and tables show the Chebyshev wavelets family, especially SCWs, is good for an approximate PDESK solution. Since most elements of derived matrices in the scheme are zeros, the computing time is short. The key advantage of the constructed scheme is that it can obtain results with high accuracy using fewer collocation nodes. The approximated PDESK solutions are provided in the form of graphs and tables. The obtained solution for the given examples shows that this scheme perfectly approximates the existing exact solution. The developed scheme is simple to implement.

9. Acknowledgement

The authors are very grateful to the editor and reviewer for carefully reading the manuscript and giving valuable suggestions, which significantly contributed to the presentation of the manuscript.

10. References

Alomari, A.K., Noorani, M.S., & Nazar, R. (2009). Solution of delay differential equation by means of homotopy analysis method. *Acta Applicandae Mathematicae*, 108(2), 395-412.

Anakira, N.R., Alomari, A.K., & Hashim, I. (2013). Optimal homotopy asymptotic method for solving delay differential equations. *Mathematical Problems in Engineering*, Article ID 498902.

Asma, Rahman, G.u., & Gómez-Aguilar, J.F. et al. (2022). Study of Multi-Term Pantograph Differential Equations of Arbitrary Order. *Few-Body Syst* 63, 71. <https://doi.org/10.1007/s00601-022-01770-0>

Azodi, H.D., & Yaghouti, M.R. (2018). A new method based on fourth kind Chebyshev wavelets to a fractional order model of HIV infection of CD4⁺T cells. *Computational Methods for Differential Equations*, 6(3), 353-371.

Bahmanpour, M., Tavassoli Kajani M., & Maleki, M. (2018). A Muntz wavelets collocation method for solving fractional differential equations. *Comp. Appl Math*, 37, 5514-5526.

Bahsi, M.M., & Cevik, M. (2015). Numerical Solution of Pantograph-Type Delay Differential Equations Using Perturbation-Iteration Algorithms. *Journal of Applied Mathematics*, Article ID 139821, 10 pages. <http://dx.doi.org/10.1155/2015/139821>.

Baker, C.T.H., Paul, C.A.H., & Wille, D.R. (1995). Issues in the numerical solution of evolutionary delay differential equations. *Advances in Computational Mathematics*, 3, 171-196.

Bellen, A., & Zennaro, M. (2003). *Numerical Methods for Delay Differential Equations*. Numerical Mathematics and Scientific Computations Series, Oxford University Press, Oxford.

Daubechies, I. (1988). Orthonormal bases of compactly supported wavelets. *Comm. Pure Appl Math*, 41, 909-996.

Drfel, G., & Iserles, A. (1997). The pantograph equation in the complex plane. *J Math Anal Appl*, 213, 117-132.

Driver, RD (1977). *Ordinary and Delay Differential Equations*. Applied Mathematics Series, Springer, New York.

Fox, L., Mayers, D.F., Ockendon, J.R., & Tayler, A.B. (1971). On a functional differential equation. *IMA Journal of Applied Mathematics*, 8(3), 271-307.

- Hafshejani, M.S., Vanani, S.K., & Hafshejani, J.S. (2011). Numerical solution of Delay Differential Equations Using Legendre Wavelet Method. *World Applied Sciences Journal*, 13, 27-33.
- Jafari, H., Mahmoudi, M. & Noori Skandari, M.H. (2021). A new numerical method to solve pantograph delay differential equations with convergence analysis. *Adv Differ Equ*, 129. <https://doi.org/10.1186/s13662-021-03293-0>
- Javadi, S., Babolian, E., & Taheri, Z. (2016). Solving generalized pantograph equations by shifted orthonormal Bernstein polynomials. *Journal of Computational and Applied Mathematics*, 303, 1-14.
- Kajani, M.T., HadiVencheh, A., & Ghasemi, M. (2009). The Chebyshev wavelets operational matrix of integration and product operation matrix. *International Journal of Computer Mathematics*, 86(7), 1118-1125.
- KarimiVanani, S., & Aminataei, A. (2010). On the numerical solution of delay differential equations using multiquadric approximation scheme. *J Functional Differential Equations*, 17, 391-399.
- Mallat, S. (2008). *A wavelet tour of signal processing: the sparse way*, Academic press, 3rd edition.
- Muhammad, A.I., Muhammad, S., Syed, T.M.D., & Muhammad, R. (2017). Modified wavelets-based algorithm for nonlinear delay differential equations of fractional order. *Advances in Mechanical Engineering*, 9, 1-8. DOI: 10.1177/1687814017696223.
- Ockendon, J.R., & Tayler, A.B. (1971). The dynamics of a current collection system for an electric locomotive. *Proc Roy Soc Lond A*, 322, 447-468.
- Rahimkhani, P., Ordokhani, Y., & Babolian, E. (2016). Numerical solution of fractional pantograph differential equations by using generalized fractional-order Bernoulli wavelet. *Journal of Computational and Applied Mathematics*, 309, 493-510.
- Rayal, A., Tamta, S., Rawat, S., & Kashif, M., (2022). Numerical view of Lucas-Lehmer polynomials with its characteristics *Uttaranchal Journal of Applied and Life Sciences*, Uttaranchal University, 3(1), 66-75.
- Rayal, A., & Verma, S.R. (2020a). An approximate wavelets solution to the class of variational problems with fractional order. *Journal of Applied Mathematics and Computing*, 65, 735-769.
- Rayal, A., & Verma, S.R. (2020b). Numerical analysis of pantograph differential equation of the stretched type associated with fractal-fractional derivatives via fractional order Legendre wavelets. *Chaos, Solitons Fractals*, 139(1), 110076.
- Rayal, A., & Verma, S.R. (2020c). Numerical study of variational problems of moving or fixed boundary conditions by Muntz wavelets. *Journal of Vibration and Control*, 28, 1-16.
- Rayal, A., & Verma, S.R. (2022). Two-dimensional Gegenbauer wavelets for the numerical solution of tempered fractional model of the nonlinear Klein-Gordon equation. *Applied Numerical Mathematics*, 174, 191-220.
- Rayal, A., (2023a). An effective Taylor wavelets basis for the evaluation of numerical differentiations. *Palestine Journal of Mathematics*, 12(1), 551-568.
- Rayal, A., Joshi, B.P., Pandey, M., & Torres, D.F.M. (2023b). Numerical Investigation of the Fractional Oscillation Equations under the Context of Variable Order Caputo Fractional Derivative via Fractional Order Bernstein Wavelets. *Mathematics*, 11(11), 2503; <https://doi.org/10.3390/math11112503>
- Rayal, A., Anand, M., Chauhan, K., & Prinsa (2023c). An Overview of Mamadu-Njoseh wavelets and its properties for numerical computations. *Uttaranchal Journal of Applied and Life Sciences*, Uttaranchal University, 4(1), 1-8.
- Rayal, A. (2023d) Muntz Wavelets Solution for the Polytropic Lane–Emden Differential Equation Involved with Conformable Type Fractional Derivative. *Int. J. Appl. Comput. Math* 9, 50; <https://doi.org/10.1007/s40819-023-01528-0>
- Saadatmandi, A., & Dehghan, M. (2009). Variational iteration method for solving a generalized pantograph equation. *Computers and Mathematics with Applications*, 58, 2190-2196.
- Saeed, U., & Rehman, M.U. (2014). Hermite Wavelet Method for Fractional Delay Differential Equations. *Journal of Difference Equations*, Article ID 359093, 1-8.
- Sedaghat, S., Ordokhani, Y., & Dehghan, M. (2012). Numerical solution of the delay differential equations of pantograph type via Chebyshev polynomials. *Communications in Nonlinear Science and Numerical Simulation*, 17, 4815-4830.
- Sezer, M., & Akyuz-Dascioglu, A. (2007). A Taylor method for numerical solution of generalized pantograph equations with linear functional argument. *Journal of Computational and Applied Mathematics*, 200, 217-225.
- Shiralashetti, S.C., Kumbinaraiah, S., Mundewadi, R.A., & Hoogar, B.S. (2016). Series solutions of pantograph equations using wavelets. *Open Journal of Applied & Theoretical Mathematics*, 2(4), 505-518.
- Tayler, A.B. (1986). *Mathematical Models in Applied Mathematics*. Clarendon Pres, Oxford, 40-53.

Tohidi, E., Bhrawy, A.H., & Erfani, K. (2013). A collocation method based on Bernoulli operational matrix for numerical solution of generalized pantograph equation. *Applied Mathematical Modelling*, 37, 4283-4294.

Tural-Polat, S.N. (2019). Third-kind Chebyshev Wavelet Method for the Solution of Fractional Order Riccati Differential Equations. *Journal of Circuits, Systems and Computers*, 28(14), 1950247.

Wang, L.P., Chen, Y.M., Liu, D.Y., & Boutat, D. (2019). Numerical algorithm to solve generalized fractional pantograph equations with variable coefficients based on shifted Chebyshev polynomials. *International Journal of Computer Mathematics*, 96, 2487-2510.

Yalcinbas, S., Aynigul, M., & Sezer, M. (2011). A collocation method using Hermite polynomials for approximate solution of pantograph equations. *Journal of the Franklin Institute*, 348, 1128-1139.

Yalcinbas, S., Sorkun, H.H., & Sezer, M. (2015). A numerical method for solutions of pantograph type differential equations with variable coefficients using Bernstein polynomials. *New Trends in Mathematical Sciences*, 3(4), 179-195.

Yang, C., (2018). Modified Chebyshev collocation method for pantograph-type differential equations. *Appl Numer Math*, 134, 132-144.

Yusufoglu, E. (2010). An efficient algorithm for solving generalized pantograph equations with linear functional argument. *Applied Mathematics and Computation*, 217, 3591-3595.

Yuzbas, S., Gok, E., & Sezer, M. (2014). Laguerre matrix method with the residual error estimation for solutions of a class of delay differential equations. *Mathematical Methods in the Applied Sciences*, 37(4), 453-463.

Zhu, L., & Wang, Y. (2013). Second Chebyshev wavelet operational matrix of integration and its application in the calculus of variations. *International Journal of Computer Mathematics*, 90(11), 2338-2352.